Copper(II) Complexes of Bis(1,4,7-triazacyclononane) Ligands with Polymethylene Bridging Groups: An Equilibrium and Structural Study

Reem Haidar, Manus Ipek, Barnali DasGupta, Mohammed Yousaf, and Leverett J. Zompa*

Department of Chemistry, University of Massachusetts at Boston, 100 Morrissey Boulevard, Boston, Massachusetts 02125-3393

Received January 22, 1997[⊗]

Copper(II) complexation by a series of ligands containing two 1,4,7-triazacyclononane, [9]aneN_3, groups conjoined by polymethylene chains two to six carbons in length is described. Equilibrium modeling studies in aqueous solution using pH−potentiometry indicate that the smallest homologue of the series, EM2, forms only $Cu(EM2)^{2+}$ in dilute aqueous solutions. All other ligands of the series form stable 1:1 (protonated and nonprotonated) and 2:1 dicopper(II) (hydroxo and non-hydroxo) complexes. Those ligands that contain bridging chains of four or more carbon atoms likely form dimeric or oligomeric complex species in solution. The EM ligands with the shortest polymethylene bridging groups form the most stable 1:1 species. There is little difference among the ligands ($n = 3-6$) in complex stability of the protonated, $CuH_2(EMn)^{4+}$, and dicopper(II), $Cu_2(EMn)^{4+}$, species. UV−vis spectroscopic continuous variation studies at pH 4.0 and 7.5 are interpreted on the basis of the principal equilibrium species obtained from the equilibrium models. Single-crystal X-ray diffraction studies on four complexes ($[Cu(EM2)]SO_4 \cdot 6H_2O$ (**1**), $[Cu_2(EM2)Cl_4] \cdot 2H_2O$ (**2**), $[Cu_2(EM6)Cl_4]$ (**3**), and $[Cu(EM3)][ZnBr_4] \cdot H_2O$ (**4**)) characterize structural features of several 1:1 monomeric and dicopper(II) complexes in the crystalline solid. The monomeric compounds contain CuN_6 chromophores while the dicopper(II) compounds contain square pyramidal CuN_3Cl_2 coordination geometry. Compound **1** crystallizes in space group $P\bar{1}$ with $a = 7.849(2)$ Å, $b = 9.783(2)$ Å, $c = 16.919(5)$ Å, $\alpha = 78.42(3)°$, $\beta = 85.76(3)°$, $\gamma = 73.06(3)°$, and $Z = 2$. **2**: $P2_1/n$ with $a = 9.689(3)$ Å, $b = 11.733(3)$ Å, $c = 10.124(3)$ Å, $\beta = 98.20(2)°$, and $Z = 2$. **3**: $P2_1/n$ with $a = 7.278(2)$ Å, $b = 12.416(3)$ Å, $c = 13.781(2)$ Å, $\beta = 90.15(2)°$, and $Z = 2$. **4**: $P2_1/c$ with $a = 9.295(3)$ Å, $b = 16.233(4)$ Å, $c = 16.544(5)$ Å, $\beta = 92.62(2)°$, and $Z = 4$. Cyclic voltammograms of aqueous solutions prepared by dissolving $[Cu_2(EM2)Cl_4] \cdot 2H_2O$ confirm its dissociation to $Cu(EM2)^{2+}$. Aqueous solutions containing 1:1 molar ratios of Cu(II) and EM2 in 0.1 mol dm^{-3} KCl at 25 °C show a one-electron chemically reversible reduction at scan rates of 500 mV s^{-1} with $E_{1/2}$ (Cu(II)−Cu(I)) = −868 mV relative to SCE. EPR (X- and Q- band) spectra of frozen solutions (1:1 DMSO/H_2O and glycerol/H_2O) of $Cu(EM2)^{2+}$ at 100 K are typical of axial copper(II) features (X-band parameters: $g_{\|} = 2.225$ ($A_{\|} = 164 \times 10^{-4}$) and $g_{\perp} = 2.045$).

Introduction

Study of bi- and polynuclear metal complexes is one of the most active areas in coordination chemistry. These compounds are used in modeling studies for important biological molecules such as metalloproteins.[1] Other areas where such compounds are being studied include multimetal-centered catalysis and oxidation−reduction.[2]

The ligands that comprise two 1,4,7-triazacyclononane ([9]-aneN_3) moieties tethered by various bridging groups provides an excellent motif to study the variation of chemical properties of binuclear complexes as changes are introduced into the ligand framework. With [9]aneN_3 as the coordinating functionality variations of ligand structure can be made without dramatically influencing the metal binding sites. Several studies of binuclear copper(II) complexes of such ligands have now appeared in the literature, and their potential as biological model compounds has been demonstrated.[3]

The compounds that contain simple polymethylene bridges provide a good starting point for systematic study of binuclear complexes. The distances between metals in the complexes can be adjusted by simply changing the length of the C atoms in the chain. In addition to possessing electronic and magnetic properties that may elucidate features found in polynuclear biological molecules, the binuclear complexes of these compounds may be expected to be excellent examples of bimetallic reaction centers.

Our studies focus on the stability of the Cu(II) complexes of these ligands in aqueous solution. Accompanying X-ray crystallographic studies indicate the stereochemistry of the complexes in the crystalline solid and provide important information about probable solution structure. The work described is a continuation of that previously reported on the Cu(II) complexes of the ligand series that contains the two [9]-aneN_3 macrocycles bridged by polymethylene chains containing

[⊗] Abstract published in *Advance ACS Abstracts,* June 15, 1997.

(1) (a) Lippard, S.; Berg, J. *Principles of Bioinorganic Chemistry*; University Science Books: Mill Valley, CA, 1994. (b) Sessler, J.; Sibert, J. *Tetrahedron* **1993**, 49, 8727 and references therein. (c) Esteruetas, M.; Garcia, M.; Lopez, A.; Ovo, A. *Organometallics* **1991**, *10*, 127 and references therein. (d) Collin, J.-P.; Jouaita, A.; Sauvage, J.-P. *Inorg. Chem.* **1988**, *27*, 1986. (e) Casellato, U.; Vigato, P.; Fenton, D.; Vidali, M. *Chem. Soc. Rev.* **1979**, 199.

(2) (a) Young, M.; Chin, J. *J. Am. Chem. Soc.* **1995**, *117*, 10577. (b) Mochizuki, K.; Gotoh, H.; Suwabe, M.; Sakahibara, T. *Bull. Chem. Soc. Jpn.* **1991**, *64*, 1750. (c) McAuley, A.; Subramanian, S.; Whitcombe, T. *J. Chem. Soc., Chem. Commun.* **1987**, 539.

(3) (a) Sessler, J.; Sibert, J.; Lynch, V. *Inorg. Chem.* **1990**, *29*, 4143. (b) Hanke, D.; Wieghardt, K; Nuber, B.; Lu, R.; McMullan, R.; Kotzle, T.; Bau, R. *Inorg. Chem.* **1993**, *32*, 4300. (c) Geilenkirchin, A.; Neubold, P.; Schneider, R.; Wieghardt, K.; Flörke, U.; Haupt, H.; Nuber, B. *J. Chem. Soc., Dalton Trans.* **1994**, 457. (d) Behle, L.; Neuburger, M.; Zehnder, M.; Kaden, T. *Helv. Chim. Acta* **1995**, *78*, 693. (e) Sessler, S.; Sibert, J.; Lynch, J.; Markert, J.; Wooten, C. *Inorg. Chem.* **1993**, *32*, 621. (f) Sessler, J.; Sibert, J.; Burrell, A.; Lynch, J.; Markert, J.; Wooten, C. *Inorg. Chem.* **1993**, *32*, 4277. (g) Blake, A.; Donlevey, T.; England, P.; Fallis, I.; Parsons, S.; Ross, S.; Schröder, M. *J. Chem. Soc., Chem. Commun.* **1994**, 1981. (h) Brudenall, S.; Spiccia, L.; Tiekink, R. *Inorg. Chem.* **1996**, *35*, 1974.

S0020-1669(97)00070-0 CCC: $14.00

three and four atoms.[4] The stability of both the mononuclear and binuclear complexes of these ligands with Cu(II) has been examined in aqueous solution by pH−potentiometric equilibrium and supporting UV−vis spectroscopic continuous variation experiments. X-ray crystallographic structural studies are reported for four complexes including two monomeric structures that contain the shorter chain ligands EM2 and EM3 and two dimeric complexes.[5] CV electrochemical and EPR studies are also reported for the Cu(II)−EM2 complexes.

Experimental Section

1,4,7-Triazacyclononane, [9]aneN_3, was either prepared by published methods[6] or purchased from Aldrich. The synthesis of 1,4,7-triazatricyclo[5.2.1.0^{4,10}]decane (**1**) was previously described.[4,7] Infrared spectra were recorded on a Perkin-Elmer 1600 FTIR. NMR spectra were recorded on a Brucker AC200, and mass spectra, on a Finnegan 8200 instrument. Magnetic susceptibilities were measured at 20 °C by the Faraday method on a Cahn Model 7600 system. The instrument was calibrated with $Hg(Co(NCS)_4)_2$.

1,1′-(Ethylene)bis(1-azoniatricyclo[2.2.2.1^{1,4}]decane) Dibromide (2a).[3b] To a stirred solution under nitrogen containing 3.75 g (26.9 mmol) of **1** in 50 mL of acetonitrile was added 2.53 g (13.5 mmol) of 1,2-dibromoethane in 10 mL of acetonitrile. The solution was stirred under a nitrogen atmosphere for 7 days. The pale yellow salt that formed was collected by filtration and washed with anhydrous acetonitrile. Yield: 62%. This material was used in the next step without further purification.

1,1′-(Pentamethylene)bis(1-azoniatricyclo[2.2.2.1^{1,4}]decane) Diiodide (2b) and **1,1′-(Hexamethylene)bis(1-azoniatricyclo[2.2.2.1^{1,4}]-decane Diiodide (2c).** To a stirred solution under nitrogen containing 20.0 mmol of **1** in 100 mL of acetonitrile was added 10.0 mmol of the appropriate diiodoalkane in 20 mL of acetonitrile. The solution was stirred under a nitrogen atmosphere for 5 days. The off-white solid that formed was removed by filtration. Yield: 80%. **2a**: Mp 265−267 °C dec; IR (KBr, cm^{-1}) 2943, 2884, 1467, 1384, 1161, 1084, 709. **2b**: Mp 253−255 °C dec; IR (KBr, cm^{-1}) 2928, 2853, 1670, 1466, 1359, 1309, 1116.

1,2-Bis(1,4,7-triaza-1-cyclononyl)ethane, EM2 (3a), 1,5-Bis(1,4,7-triaza-1-cyclononyl)pentane, EM5 (3b), and 1,6-Bis(1,4,7-triaza-1-cyclononyl)hexane, EM6 (3c). The base hydrolysis follows the procedure reported for EM3 and EM4.[4] A 150 mL aqueous solution containing 10 mmol of the dibromide or diiodide salt (**3a**−**c**) was refluxed under a nitrogen atmosphere for 2 h. Solid (0.15 mol) NaOH was cautiously added and the refluxing continued for an additional 8 h. After cooling, the reaction mixture was extracted four times with 30 mL portions of $CHCl_3$. The combined extracts were dried over Na_2SO_4 (anhydrous). After filtering and removal of the solvent in vacuo, a pale yellow oil remained. This material was Kugelrohr distilled (160 °C, 0.050 mmHg), giving a colorless oil that solidified upon cooling in the refrigerator. **3a**: Yield 80%; ^{1}H NMR δ 2.51 (4H, br, NH), 2.64−2.70 (28H, m, CH_2) (lit.[8] δ 2.17, 2.68); ^{13}C NMR δ 45.99, 46.26, 52.80, 56.03. **3b**: Yield 63%; ^{1}H NMR δ 1.25 (2H, br, CH_2), 1.40 (4H, br, CH_2), 2.10 (4H, br, NH), 2.44−2.51 (12H, m, $N(CH_2)_3$), 2.63−2.68 (16H, m, $NH(CH_2)_2$); ^{13}C NMR δ 25.32, 27.95, 46.76, 53.00, 53.30, 57.79; EI MS *m*/*e* 326.4 (M^+) (calcd for $C_{17}H_{38}N_6$, *m*/*e* 326.3). **3c**: Yield 62%; ^{1}H NMR δ 1.30 (4H, br, −CH_2), 1.42 (4H, br, −CH_2), 2.53 (12H, m, $N(CH_2)_3$), 2.80 (20H, m, $NH(CH_2)_2$ and NH); ^{13}C NMR δ 27.39, 27.94, 46.34, 46.52, 52.76, 57.70; EI MS *m*/*e* 340.3 (M^+) (calcd for $C_{18}H_{40}N_6$, *m*/*e* 340.3).

Hydrochloride Salts of 3a−c. Concentrated hydrochloric acid (10 mL) was added to a solution of the amine (3.5 mmol) in 2−3 mL of water. After cooling in an ice-water bath, the off-white solid that formed was collected by filtration. The solid was redissolved in hot hydrochloric acid (3 mol dm^{-3}) containing a small amount of activated carbon. The carbon was removed by filtration, and upon cooling in an ice-water bath, the white hydrochloride salt precipitated. Yield: >90%. The salts were dried in vacuo at 40 °C. Anal. Calcd for $C_{14}H_{40}N_6Cl_6O$ (mol wt 521.2) (EM2·6HCl·H_2O): C, 32.26; H, 7.74; N, 16.12; Cl, 40.81. Found: C, 32.13; H, 7.74; N, 16.06; Cl, 41.30. Anal. Calcd for $C_{17}H_{52}N_6Cl_6O_4$ (mol wt 617.4) (EM5·6HCl·$4H_2O$): C, 33.07; H, 8.49, N, 13.61; Cl, 34.46. Found: C, 33.34; H, 8.39; N, 13.62; Cl, 34.02. Anal. Calcd for $C_{18}H_{54}N_6Cl_6O_4$ (mol wt 631.4) (EM6·6HCl·$4H_2O$): C, 34.24; H, 8.62; N, 13.31; Cl, 33.69. Found: C, 34.11; H, 8.16; N, 13.41; Cl, 33.85.

[Cu(EM2)]SO_4·0.5H_2O and [Cu(EM2)]SO_4·6H_2O. The pH of a solution containing equimolar quantities of $CuSO_4$ (0.13 mmol) and EM2·6HCl (0.68 g, 0.13 mmol) in 3 mL of water was adjusted to 6−7 with NaOH solution. The solution was warmed to 50 °C and 2−3 mL of DMSO added. Upon cooling, blue crystals of the hemihydrate complex form. Anal. Calcd for $C_{14}H_{33}N_6SO_{4.5}Cu$ (mol wt 453.1): C, 37.12; H, 7.34; N, 18.55, S, 7.1. Found: C, 37.20, H, 7.18, N, 18.54; S, 7.6. Crystals suitable for X-ray crystallography were grown on microscope slides by slow cooling of DMSO/water solutions containing the above complex. The results of the X-ray study show the crystals obtained on the slide to be a hexahydrate.

The value of the magnetic moment measured at 20 °C is 2.0 μ_B.

[Cu(EM3)]$ZnBr_4$·H_2O. A solution containing EM3[4] (0.075g., 0.25 mmol), $Cu(NO_3)_2$ (0.25 mmol), $Zn(NO_3)_2$ (0.25 mmol), and NaBr (1.0 mmol) in 20 mL of water was evaporated to 5 mL on a steam bath. After standing for several days, blue platelike crystals formed. Elemental analysis indicated an approximate 1:1 Cu to Zn molar ratio. These crystals were suitable for X-ray crystallographic study.

[Cu_2(EM2)Cl_4]·H_2O and [Cu_2(EM2)Cl_4]·2H_2O. An aqueous solution (10 mL) containing $CuCl_2$ (0.40 mmol) and EM2·6HCl·H_2O (0.104 g, 0.20 mmol) was adjusted to pH 6−7 by addition of 0.5 mol dm^{-3} NaOH. Evaporation on a steam bath to a small volume (1−2 mL) followed by cooling gave a blue crystalline solid. The crystals were ground and dried in vacuo at room temperature. Anal. Calcd for $C_{14}H_{34}N_6Cl_4O$ (mol wt 571.4) (Cu_2(EM2)Cl_4·H_2O): C, 29.43; H, 6.00; N, 14.71; Cl, 24.82. Found: C, 29.11; H, 6.04; N, 14.52; Cl, 24.80. Crystals of the compound suitable for X-ray crystallographic study were grown by slow evaporation of solutions containing 2:1 molar ratios of $Cu(ClO_4)_2$ and EM2 at pH 6−7. The X-ray study indicates that the dihydrate salt is obtained in this manner.

[Cu_2(EM6)Cl_4]. This compound was synthesized in a manner similar to that for the EM2 compound above. Slow evaporation of aqueous solutions produced X-ray-quality crystals. Anal. Calcd for $C_{18}H_{36}N_6Cu_2Cl_4$ (mol wt 605.4) (Cu_2(EM6)Cl_4): C, 35.71; H, 5.99; N, 13.88; Cl, 23.42. Found: C, 35.22; H, 6.74; N,13.73; Cl, 23.41.

Cu(EM6)$(NO_3)_2$·3.5H_2O. The addition of a 10-fold molar excess of KNO_3 (0.1 mol dm^{-3}) to solutions containing equimolar quantities (0.01 mol dm^{-3}) of $Cu(NO_3)_2$ and EM6 at pH 6−7 produces a violet colored powder that after filtering and drying analyzes as a hydrate of the 1:1 complex. Anal. Calcd for $C_{18}H_{47}N_8O_{9.5}Cu$ (mol wt 591.2) (Cu(EM6)$(NO_3)_2$·3.5H_2O): C, 36.57; H, 8.01; N, 18.95; Cu, 10.7. Found: C, 36.43; H, 7.21; N, 19.42; Cu 10.5.

pH−Potentiometric Titrations. The pH measurements were made with a Beckman Model Φ71 pH meter fitted with Fisher glass and Ag/AgCl reference electrodes by methods previously described.[4] In cases where attainment of equilibrium was very slow (>1 h) an automated pH-meter/buret system was used.[9] This device consisted of Radiometer Model PHM62 meter with an Orion combination glass and Ag/AgCl electrode (91-05) to monitor pH. The pH meter output is digitized and interfaced with a computer. A computer program monitors the pH change with time and when constant, as defined by an algorithm that evaluates ΔpH/Δt, triggers a Fisher Model 395 digital buret to add a fixed increment of titrant. Using this device allows collection of pH−potentiometric data for periods of several days. Calibration checks indicate that the pH drift of the meter/electrode system over a period of 3 days is usually less than ±0.02 pH units.

Titrations were performed in a sealed thermostated (25.0 °C) cell under a blanket of presaturated nitrogen. The meter−electrode system

(4) Zhang, X.; Hsieh, W.-Y.; Margulis, T.; Zompa, L. *Inorg. Chem.* **1995**, *34*, 2883.
(5) The ligands are designated by the symbol EM*n*, where the *n* refers to the length of the C chain in the bridge joining the [9]aneN_3 groups.
(6) (a) Richman, J.; Atkins, T. *J. Am. Chem. Soc.* **1980**, *21*, 3635. (b) Parker, D. *Macrocycle Synthesis*; Parker, D., Ed.; Oxford Univ. Press: Oxford, England, 1996.
(7) Weisman, G.; Vachon, D.; Johnson, V.; Gronbeck, D. *J. Chem. Soc., Chem. Commun.* **1987**, 886.
(8) Wieghardt, K.; Tolksdorf, I.; Herrmann, W. *Inorg. Chem.* **1985**, *24*, 1230.
(9) Volpicelli, R.; Zompa, L. Manuscript in preparation.

was calibrated with 4.008 buffer at 25 °C. Meter correction was made by measuring the pH of a 0.00100 M HCl which was 0.1 M in KNO_3. The value measured was used to compute a correction factor by assuming that the pH of 0.001 00 M H^+ was 3.000. Linearity was checked with 0.0100 M HCl and 0.0100 M NaOH solutions both 0.1 M in KNO_3. The value of pK_w was 13.797.

Preparation of ligand and Cu(II) solutions and procedures were previously described.[4] The concentrations of solutions studied ranged from 0.001 to 0.007 M.

Equilibrium Calculations. Analysis of the pH potentiometric data was done with the computer programs SCOGS2[10] and SUPERQUAD.[11] The methodology for equilibrium modeling is presented in an earlier paper.[4] Formation constants presented in the tables were computed with data from at least 8 different titrations for each Cu(II)−ligand system. Average deviations of the constants are given along with the standard deviations. Standard deviations of constants for a single titration were always smaller than those given in the table. Statistical data from both SCOGS and SUPERQUAD were well within acceptable limits.

Spectrophotometric Studies. Continuous variation spectrophotometric studies with Cu(II) were done for each ligand at pH 4.0 and 7.5. In a typical experiment nine solutions containing Cu(II) and EM*n*·6HCl ($n = 2-6$) in molar ratios ranging from 0.25:1 to 2.25:1 were prepared. Before final dilution in volumetric flasks the pH of each solution was adjusted to 4.0 by addition of NaOH solution. The ionic strength of each solution was 0.10 M (KNO_3), and UV−vis spectra were recorded at 25 °C. Ligand concentration (4−8 mmol dm^3) was held constant for each series of measurements. Aliquots of these solutions were adjusted to pH 7.5 by addition of NaOH solution and appropriately diluted. UV−vis spectra of these solutions provided data sets at pH 7.5 ± 0.1.

Cyclic Voltammetry. All electrochemical experiments were carried out in a three-electrode cell thermostated at 25 °C under an atmosphere of argon. Cyclic voltammograms were obtained with a BAS Model 100 B/W electrochemical work station. A glassy carbon (2 mm) electrode was used as the working electrode. A platinum wire auxiliary electrode and a saturated calomel reference (SCE) completed the electrode system.

Electron Paramagnetic Resonance Studies. EPR measurements on [Cu(EM2)]SO_4 (10^{-3} mol dm^{-3}) in frozen solutions (water−glycerol (1:1) or water−DMSO (1:1)) at about 100 K were made with a Varian E9 X-band (microwave frequency 9192 GHz, field range 2500−3500 G) and Q-band (microwave frequency 34.77 GHz, field range 10 600−12 600 G) spectrometers. X-band magnetic field measurements were made with an AEG NMR field probe, and the microwave frequency was measured with an EIP Model 575B microwave counter. Magnetic measurements were made in the Q-band with a MicroNOW NMR gaussmeter, and microwave frequency parameters are reported relative to Mn(II) in CaO.

Crystallographic Studies. Cell dimensions and intensity data were measured with a Syntex $P2_1$ diffractometer using monochromated Mo Kα radiation and $\theta-2\theta$ scans. Cell dimensions were determined by least-squares refinement of 24 reflections ($25 < 2\theta < 40$). Three control reflections collected every 75 reflections showed no significant trends. Intensities were corrected for Lorentz and polarization effects. Absorption corrections were applied from ψ scans of six reflections with χ near 90° for compounds **2**−**4**.[12] For compound **1** an empirical absorption correction SHELXA90[13] was applied. Structures were solved by direct methods and refined using full-matrix least-squares techniques.

All calculations were performed with the SHELXTL PLUS suite of computer programs.[14] Final refinements employed SHELXL93.[13] Unit cell parameters and a summary of data collection and refinement are given in Table 4.

(10) Perrin, D.; Stunzi, H.; *Computational Methods for the Determination of Formation Constants*; Plenum: New York, 1985.
(11) Gans, P.; Sabatini, A.; Vacca, A. *J. Chem. Soc., Dalton Trans.* **1985**, 1195.
(12) XDISK. *Data Reduction Program*; Ver. 3.13, Siemens Analytical X-Ray Instruments, Inc.: Madison, WI, 1989.
(13) Sheldrick, G. SHELXL93. *Program for the Refinement of Crystal Structures*; Univ. of Göttingen, Göttingen, Germany.
(14) Sheldrick, G. *SHELXLTL-PLUS*; Siemens Analytical X-Ray Instruments, Inc.: Madison, WI, 1990.

Table 1. Acid Dissociation Constants for Protonated Forms of the Ligands (EM*n*) at 25 °C in 0.10 mol dm^{-3} KNO_3

	− log K_a				
reacn	EM2	EM3[b]	EM4[b]	EM5	EM6
$HL^+ \rightleftarrows L + H^+$	11.21(2)	11.08(5)	11.21(3)	11.24(3)	11.26(2)
$H_2L^{2+} \rightleftarrows HL^+ + H^+$	10.18(5)	10.38(4)	10.48(3)	10.50(3)	10.52(3)
$H_3L^{3+} \rightleftarrows H_2L^{2+} + H^+$	6.31(2)	6.47(2)	6.57(3)	6.64(2)	6.66(2)
$H_4L^{4+} \rightleftarrows H_3L^{3+} + H^+$	5.60(4)	5.77(2)	5.87(2)	5.98(2)	6.03(4)

[a] Estimated standard deviations in parentheses. [b] Reference 4.

[Cu(EM2)]SO_4·6H_2O (1). All hydrogens were found on difference maps. The hydrogens on C and N were introduced in calculated positions, and those on the water molecules were placed at positions determined from difference maps. The hydrogens were refined isotropically with fixed $U = 0.08$ Å. Final difference Fourier maps showed largest deviations of 0.64 and −0.83 e $Å^{-3}$ near Cu(II).

[Cu_2(EM2)Cl_4]·2H_2O (2). All hydrogens were found on difference maps and refined as described above. Largest deviations in the final difference map are 0.41 and −0.59 e $Å^3$.

[Cu_2(EM6)Cl_4] (3). All hydrogens were found on difference maps and refined as described above. Largest deviations in the final difference map are 0.42 and −0.45 e $Å^{-3}$.

[Cu(EM3)]$ZnBr_4$·H_2O (4). All heavy atoms were refined anisotropically. Hydrogen atoms on the ligand were placed in ideal positions (0.96 Å for C−H and 0.90 Å for N−H bonds) and refined using the "ride approximation". There appears to be some disorder associated with the $ZnBr_4^{2-}$, but various models used did not improve the structure. The mean square atomic displacements for several C atoms, especially in the bridge (C(13) and C(14)), and the O atom are also large. These factors likely contribute to the large value of R_f. The hydrogens associated with the water molecule were not found on difference maps and were not calculated.

Results and Discussion

Acid Dissociation of H_6(EM*n*)$^{6+}$ ($n = 2-6$). The acid dissociations of the hexahydrochloride salts of the EM*n* ($n = 2-6$) amines follow similar trends: two strong, two moderately weak, and two weak acid dissociations. For each dissociation the relative invariance in magnitude of pK_a between the compounds indicates that the two strong acid protons are likely associated with the tertiary amine nitrogen atoms.[4] The crystal structure of H_4(EM2)$^{4+}$ in the salt [H_4(EM2)$^{4+}$][$CdCl_4^{2-}$]$_2$ where protons are strongly hydrogen bonded to the secondary amine nitrogens presents additional support for this argument.[15] The acid dissociation constants for the protonated ligands are given in Table 1.

Cu(II)−EM2 Complexation. The pH−potentiometric metal complexation titration curves for Cu(II) and EM2·6HCl with NaOH show only a single inflection. The curve for 1:1 Cu(II):EM2 shows this single steep inflection at $a = 6$ (a = mol of base per mol of ligand). The position of the inflections do not change in titrations where the molar ratio of Cu(II) > EM2, but precipitates form at pH ≥ 7. Analysis of all the titration data from $a = 2.3$ to 5.7 indicates that one complex species, CuL^{2+}, predominates. The following UV−vis spectrophotometric and electrochemical experiments support this conclusion.

UV−vis spectra of solutions containing varying ratios of Cu(II) to EM2 at pH 4 have absorption maxima at 648 nm and show no change in the wavelength as [Cu^{2+}] is increased versus [EM2]. The absorbance increases linearly as [Cu^{2+}]/[EM2] is increased. The curve flattens when an equimolar ratio is reached. Experiments performed at pH 7.5 give similar results. The absorption maximum of solutions containing equimolar quantities of Cu(II) and EM2 are virtually independent of pH from 4 through 11.

(15) Zompa, L.; Haidar, R. *Acta Crystallogr.* **1996**, *C52*, 1188.

Table 2. Formation Constants for Copper(II) Complexes of the Ligands EM*n* at 25.0 °C in 0.10 mol dm^{-3} KNO_3[a]

	log β				
reacn	EM2	EM3[c]	EM4[c]	EM5	EM6
$Cu^{2+} + L \rightleftarrows CuL^{2+}$ [d]	27.82(7)	24.90(3)	23.02(6)	21.6(2)	21.3(1)
$Cu^{2+} + H^+ + L \rightleftarrows CuHL^{3+}$		27.4(1)	27.0(2)	27.2(2)	27.0(1)
$Cu^{2+} + 2H^+ + L \rightleftarrows CuH_2L^{4+}$		31.64(5)	32.02(9)	32.31(9)	32.3(1)
$2Cu^{2+} + L \rightleftarrows Cu_2L^{4+}$		29.08(7)	29.61(6)	29.64(7)	29.69(8)
$2Cu^{2+} + L \rightleftarrows Cu_2LOH^{3+}$ [b]		22.5(2)	22.9(2)	22.7(2)	22.7(2)
$2Cu^{2+} + L \rightleftarrows Cu_2L(OH)_2^{2+}$ [b]		17.0(1)	17.98(9)	17.61(8)	17.98(8)

[a] Estimated standard deviation in parentheses. [b] For hydrolysis reactions the notation for β is written as the product βK_w, which is the standard format in computer programs such as SCOGS2 and SUPERQUAD. [c] Reference 4. [d] See text.

Cyclic voltammetry was done in aqueous 0.1 mol dm^{-3} KCl at 25 °C at pH 6. Solutions containing equimolar quantities of Cu(II) and EM2 show a one-electron chemically reversible reduction at scan rates of 500 mV s^{-1} with $E_{1/2}$ (Cu(II)−Cu(I)) = −868 mV (ΔE_p = 86 mV) relative to the standard calomel electrode. CVs of solutions prepared by adding $[Cu_2(EM2)Cl_4]\cdot 2H_2O$ to 0.1 mol dm^{-3} KCl at similar conditions produce a more complicated curve but show a reduction at −862 mV. The portion of the CV at more positive potentials is virtually identical to that of a solution containing Cu(II) in the same medium. Thus, it appears that the addition of solids containing $Cu_2(EM2)^{4+}$ to water at these conditions results in dissociation to $Cu(EM2)^{2+}$ and Cu(II).

Cu(II)−EM*n* (*n* = 3−6) Complexation. The EM5 and EM6 complexation with Cu(II) more closely resembles EM3 and EM4 described previously.[4] Titration of 1:1 Cu(II) EM*n*·6HCl (*n* = 5, 6) solutions with NaOH give inflections at *a* = 4 and 6, while 2:1 solutions give inflections at *a* = 6 and 8. Analysis of the pH−potentiometric titration data indicates that CuH_2L^{4+}, $CuHL^{3+}$, CuL^{2+} (or $Cu_xL_x^{2x+}$), and Cu_2L^{4+} are important equilibrium species. When the Cu(II):L ratio exceeds 1:1 hydroxo species of the form Cu_2LOH^{3+} and $Cu_2L(OH)_2^{2+}$ also appear stable (pH > 8).

The formation constants for Cu(II) with the EM ligands are shown in Table 2. The most dramatic trend occurs for the 1:1 complexes. Starting with EM2, each time the chain is lengthened by one C atom the stability of the complex decreases. When the length of the chain exceeds four there is little driving force to form the mononuclear complex, CuL^{2+}. For example, the chelate ring comprising the bridge for a mononuclear $Cu(EM5)^{2+}$ species would consist of eight atoms. Equimolar species are important constituents of the equilibrium model, but in the case of the larger chain ligands these species may be dimeric or oligomeric. It is not likely that CuL^{2+} complexes contain a coordinated and a noncoordinated ring (**I**).

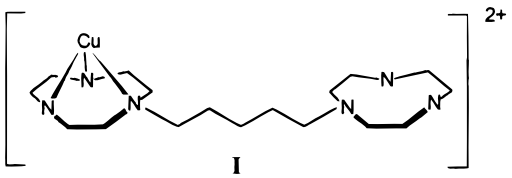

I

When aqueous salt solutions containing noncoordinating anions (NO_3^- and ClO_4-) are added to equimolar solutions containing Cu(II) and EM*n* (*n* ≥ 4) ligands at pH 6−7, fine blue or blue-violet precipitates form. These precipitates may be redissolved by addition of acid or Cu(II) to solution. Analysis of the dried precipitates indicate an approximate 1:1 stoichiometry. It is quite possible that these complexes are polymeric in nature. Salts of the monomeric complexes $(Cu(EMn)^{2+}$ (*n* = 2, 3)) and $Cu([x]aneN_3)^{2+}$ (*x* = 9−11) complexes tend to be quite soluble.[4,16] The solubility of these compounds resemble Cu(II) complexes of pentaerythityltetramine where polymeric complexes are also believed to occur.[17] Recent evidence for the existence of dimers in crystalline solids containing Ni(II) and EM5 has been provided by the X-ray crystal structure of $[Ni_2(EM5)_2](NO_3)_4$.[18]

Equilibrium modeling of the Cu(II)−EM*n* (*n* ≥ 4) systems for dinuclear, $Cu_2L_2^{4+}$ (**II**), or polynuclear, $Cu_xL_x^{2x+}$ (**III**),

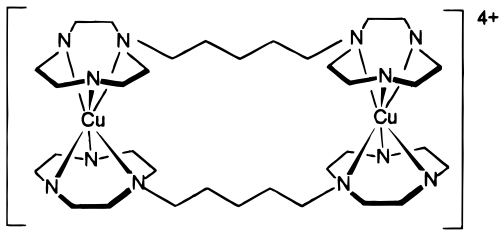

II

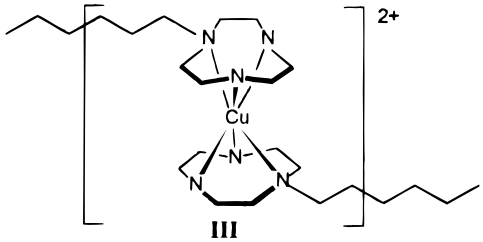

III

species is complicated by several factors: (1) The quality of the data suffers because of the long equilibrium times required. (2) Several other stable complex species exist in the pH range where these complexes form. (3) If *x* is larger than 2 or 3, modeling is, at best, approximate. Although the model is statistically less precise, it is possible for example to replace CuL^{2+} with $Cu_2L_2^{4+}$ in computational models of the 1:1 Cu(II):EM*n* (*n* = 4−6) titration data. For example, calculations for log β for $Cu_2(EM6)_2^{4+}$ give a value of 45.3. The values of log β_{CuL} in Table 2 for these ligands therefore reflect a complex with 1:1 stoichiometry and formation constants of the following form: $\log(\beta_{Cu_xL_x})/x$. The equilibrium reaction in this case will be $xCu^{2+} + xL \rightleftarrows Cu_xL_x^{2x+}$.

Formation constants for the Cu_2L^{4+} complexes are identical in magnitude within experimental error (Table 2). Such behavior indicates that regarding complex stability there is little

(16) (a) Yang, R.; Zompa, L. *Inorg. Chem.* **1976**, *15*, 1499. (b) Zompa, L. *Inorg. Chem.* **1978**, *17*, 2531.
(17) Zompa, L.; Bogucki, R. *J. Am. Chem. Soc.* **1966**, *88*, 5186.
(18) X-ray crystallographic studies on $[Ni_2(EM5)_2](NO_3)_4$ show the compound to have a sandwich structure with two Ni(II) ions coordinated between two EM5 ligands. Each ligand has a tridentate [9]aneN$_3$ coordinated to different Ni(II) ions similar to structure **II** in this paper. Refinement is down to $R(4\sigma) \approx 0.13$. Publication of this work has been delayed due to some decay of the crystals in the X-ray beam and apparent disorder among the anions. However, this does not imply that because dimers occur with Ni(II) they also occur with Cu(II).

Table 3. Equilibrium Constants for Copper(II) Complexes of the EM*n* Ligands at 25 °C in 0.1 mol dm^{-3} KNO_3 Calculated from Constants in Tables 1 and 2

		log *K*				
constant	reacn	EM2	EM3[a]	EM4[a]	EM5	EM6
$K_a(CuH_2L)$	$CuH_2L^{4+} \rightleftarrows CuHL^{3+} + H^+$		−4.2	−5.0	−5.1	−5.3
$K_a(CuHL)$	$CuHL^{3+} \rightleftarrows CuL^{2+} + H^+$		−2.5	−4.0	−5.6	−5.7
K_2	$Cu^{2+} + CuL^{2+} \rightleftarrows Cu_2L^{4+}$		4.2	6.6	8.0	8.4
$K_a(Cu_2L)$	$Cu_2L^{4+} \rightleftarrows Cu_2LOH^{3+} + H^+$		−6.6	−6.7	−6.9	−7.0
$K_a(Cu_2LOH)$	$Cu_2LOH^{3+} \rightleftarrows Cu_2L(OH)_2^{2+} + H^+$		−5.5	−5.0	−5.1	−4.7

[a] Reference 4.

Table 4. Crystallographic Data for $[Cu(EM2)]SO_4 \cdot 5H_2O$ (**1**), $[Cu_2(EM2)Cl_4] \cdot 2H_2O$ (**2**), $[Cu_2(EM6)Cl_4]$ (**3**), and $[Cu(EM3)]ZnBr_4 \cdot H_2O$ **(4)**

	1	**2**	**3**	**4**
formula	$CuC_{14}H_{44}N_6O_{10}S$	$Cu_2C_{14}H_{36}N_6Cl_4O_2$	$Cu_2C_{18}H_{40}N_6Cl_4$	$CuZnC_{15}H_{36}N_6Br_4$
fw	552.2	589.4	609.4	765.1
space group	$P\bar{1}$	$P2_1/n$	$P2_1/n$	$P2_1/c$
a, Å	7.849(2)	9.689(3)	7.278(2)	9.295(3)
b, Å	9.783(3)	11.755(3)	12.416(3)	16.233(4)
c, Å	16.919(5)	10.124(3)	13.781(2)	16.544(5)
α, deg	78.42(3)			
β, deg	85.76(3)	98.20(2)	90.15(2)	92.62(2)
γ, deg	73.06(3)			
V, Å^3	1217.1	1411.3	1244.6	2494(1)
Z	2	2	2	4
λ(Mo Kα),Å^3	0.710 73	0.710 73	0.710 73	0.710 73
cryst size, mm	0.80 × 0.38 × 0.12	0.32 × 0.30 × 0.12	0.22 × 0.18 × 0.50	0.50 × 0.40 × 0.10
T, °C	20	20	20	20
ρ_{calcd}, g·cm^{-3}	1.507	1.715	1.626	2.035
$\rho_{meas\ (floatation)}$, g·cm^{-3}	1.47	1.69	1.57	2.0
h,*k*,*l* range collcd	$0 \le h \le 11, -14 \le k \le 14, -25 \le l \le 25$	$0 \le h \le 12, 0 \le k \le 15, -13 \le l \le 13$	$0 \le h \le 19, 0 \le k \le 16, -17 \le l \le 17$	$0 \ge h \ge 12, 0 \ge k \ge 21, -22 \ge l \ge 22$
μ, cm^{-1}	10.4	23.6	21.6	8.23
transm factors	0.93/0.33	0.23/0.20	0.28/0.21	0.96/0.26
no. of unique reflns	8861	2638	2870	6316
reflns ($F > 4.0\sigma(F)$)	5751	1758	1875	3226
no. of params	421	175	195	253
w*R*2	0.118	0.113	0.115	0.199
R[b]	0.062	0.054	0.060	0.109
GOF	1.03	1.19	1.08	1.14

[a] $wR2 = [\sum w(F_o^2 - F_c^2)^2/\sum wF_o^4]^{1/2}$. [b] $R = \sum||F_o| - |F_c||/|F_o|$.

influence of one coordination site on the other. A separation of one site by as few as three C atoms has virtually the same impact as a separation of six C atoms. Thus formation of the dicopper(II) complexes, Cu_2L^{4+}, by addition of Cu^{2+} to the 1:1 complexes, CuL^{2+} or $Cu_xL_x^{2x+}$, is almost entirely dependent on the stability of the 1:1 complexes. This is seen by the increasing magnitude of log K_2 (Table 3) with length of bridging chain *n*. The relatively small magnitude of log K_2 provides further evidence for the existence of polynuclear CuL^{2+} complexes. If monomeric Cu(II) complexes of EM*n* ($n > 4$) are generally unstable, the formation constant for the reaction of Cu^{2+} with CuL^{2+} to form Cu_2L^{4+} might be expected to be only a few orders of magnitude smaller than that for the reaction Cu^{2+} + [9]aneN$_3$ ⇄ Cu([9]aneN$_3$)$^{2+}$ (log $\beta = 15.5$).[16] The calculated values are 7 log units smaller.

The trend in acidity of the protonated complexes has previously been discussed in light of the driving force for $CuHL^{3+}$ to form mononuclear CuL^{2+} complexes (L = EM*n*, $n = 3, 4$).[4] In these cases the acidity of $CuHL^{3+}$ is greater than CuH_2L^{4+}. The trend reverses for the longer chain ligands ($n = 5, 6$).

Continuous variation spectrophotometric studies done at pH 4.0 and 7.5 where [EM*n*] is fixed and [Cu^{2+}] is varied shows similar general trends for the ligands with $n = 3-6$. As [Cu^{2+}] is increased, the solution absorbance increases until [Cu^{2+}]/[EM*n*] ≅ 2. When this ratio is reached, increasing [Cu^{2+}] has little effect on the absorbance indicating the stability of the dicopper(II) complexes. However, these experiments do show a clear distinction between EM3 and its congener ligands.

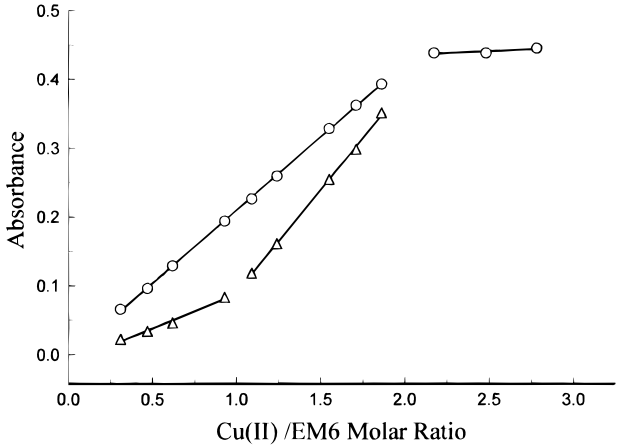

Figure 1. Absorbance at 650 nm versus [Cu^{2+}]/[EM6] at pH 4.0. Lines shown are linear least-squares lines drawn with experimental points (○) from 0.31 to 1.86 molar ratios. Absorbance at 626 nm versus [Cu^{2+}]/[EM6] at pH 7.5. Lines shown are linear least-squares lines drawn with experimental points (△) from 0.31 to 0.93 and 1.09 to 1.86 molar ratios.

For ligands with $n > 3$ the continuous variation experiments at pH 4.0 show virtually no change of λ_{max} with various [Cu(II)]/[EM*n*] ratios. Plots of A_{max} versus [Cu(II)]/[EM*n*] give straight lines for molar ratios 0.25−2.0 (Figure 1). Equilibrium studies show that CuH_2L^{4+} is dominant when [Cu(II)]/[EM*n*] ≤ 1 and Cu_2L^{4+} forms with concomitant decrease in CuH_2L^{4+} when [Cu(II)]/[EM*n*] > 1. It is likely that the coordinative geometries in solution of CuH_2L^{4+} and Cu_2L^{4+} are similar. This will result in the absorbance maximum of these complexes

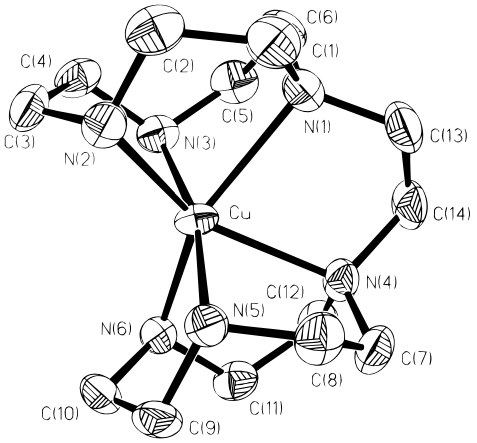

Figure 2. Thermal ellipsoid plot showing the structure of $[Cu(EM2)]^{2+}$ in $[Cu(EM2)]SO_4 \cdot 6H_2O$ (**1**). Thermal ellipsoids are at the 50% probability level.

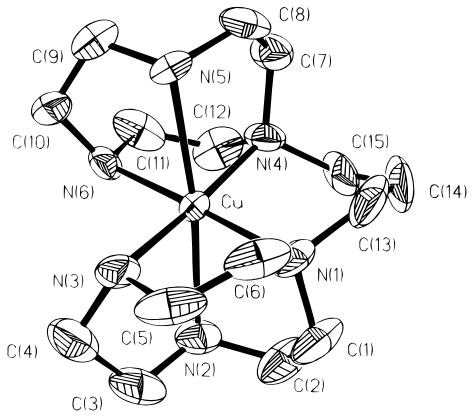

Figure 3. Thermal ellipsoid plot showing the structure of $[Cu(EM3)]^{2+}$ in $[Cu(EM3)][ZnBr_4] \cdot H_2O$ (**4**). Thermal ellipsoids are at the 50% probability level.

occurring at nearly the same wavelength. Thus, the linearity of the plots can be explained by assuming that Cu_2L^{4+} has twice the molar absorptivity of CuH_2L^{4+}. Interpretation of the data in this manner provides a means of calculating the extinction coefficients for these complexes (Table 9).

In the case of EM3 λ_{max} shifts from 643 to 613 nm as [Cu(II)]/[EM3] is varied from 2.0 to 0.25. At this acid strength (pH 4) when [Cu(II)]/[EM3] $\leq$ 1 equilibrium data show that $Cu(EM3)^{2+}$ predominates over $CuH_2(EM3)^{4+}$. When [Cu(II)]/[EM3] > 1, $Cu_2(EM3)^{4+}$ is present. Thus the shift in λ_{max} may be attributed to the difference in the Cu(II) coordination sites of $Cu(EM3)^{2+}$ and $Cu_2(EM3)^{4+}$. The extinction coefficients for these complexes are given in Table 9.

Continuous variation studies at pH 7.5 also show shifts in wavelengths of the absorbance maxima with varying metal to ligand ratios. Using EM6 as an example, λ_{max} ranges from 650 to 582 nm as $[Cu^{2+}]$/[EM6] varies from 2.25 to 0.25. A plot of A_{650nm} versus $[Cu^{2+}]$/[EM6] is a curve that is comprised of three intersecting straight lines. The slope of these lines changes at 1:1 and 2:1 molar ratios (Figure 1). (Only two lines are shown on the plot since there is no change in absorbance when the molar ratio is greater than 2:1.) Conversion from $CuH_2(EM6)^{4+}$ to a nonprotonated complex species is complete at pH 7.5 ($[Cu^{2+}]$/[EM6] $\leq$ 1). Thus, the linear portion of the continuous variation curve at low metal to ligand ratios reflects the formation of the nonprotonated 1:1 complex. As previously discussed, the nonprotonated 1:1 complexes may be dimeric or oligomeric, $Cu_xL_x^{2x+}$. Similar spectroscopic trends are observed for the EM*n* ligands where $n \geq 4$. Extinction coefficients at the absorbance maxima for $Cu_xL_x^{2x+}$ where L = EM*n* ($n > 3$) are given in Table 9. For oligomeric complexes the values represent ϵ/Cu(II).

For Cu(II) and EM3 at pH 7.5 the λ_{max} varies from 613 nm at low metal to ligand ratios and shifts to 609 nm at higher ratios. The absorbance at 613 nm may be explained by the presence of $Cu(EM3)^{2+}$ which is also the major species in the pH 4.0 study when $[Cu^{2+}]$/[EM3] < 1. Calculation of the extinction coefficient at 613 nm from the pH 7.5 data is equal within experimental error to the value calculated at pH 4.0.

The EM*n* ($n \geq 3$) ligands form hydrolyzed species at pH 7.5 when [Cu(II)]/[EM*n*] > 1. The stoichiometry of these complexes from the equilibrium data is in agreement with $Cu_2L(OH)_2^{2+}$. Extinction coefficients for these species are calculated from the data where 1 < [Cu(II)]/[EM*n*] $\leq$ 2.

X-ray Crystallographic Studies. Structures of both mononuclear and binuclear Cu(II) complexes of several of the EM complexes have been determined by X-ray crystallography. The mononuclear complexes $[Cu(EM2)]SO_4 \cdot 6H_2O$ (Figure 2) and $[Cu(EM3)]ZnBr_4 \cdot H_2O$ (Figure 3) both contain six-coordinate Cu(II). Pertinent bond distances and angles for these compounds are listed in Tables 5 and 6. The structures are similar to the extent that the coordination polyhedra show distortions typical of d^9 CuN_6 chromophores with two long Cu−N bonds ranging from 2.30 to 2.41 Å and four Cu−N bonds with lengths varying between 2.04 and 2.11 Å. Imposed on this is a trigonal distortion about a pseudo-C_3-axis through the Cu atom and normal to each of the planes formed by the N atoms of the two nine-membered rings. Intra-ring N−Cu−N bond angles ranging from 79.4 to 83.7° indicate the magnitude of the trigonal distortion.

Table 5. Selected Bond Distances (Å) and Angles (deg) for $[Cu(EM2)]SO_4 \cdot 6H_2O$

Cu−N(1)	2.347(3)	N(5)−C(8)	1.480(4)
Cu−N(2)	2.098(3)	N(5)−C(9)	1.486(4)
Cu−N(3)	2.084(3)	N(6)−C(10)	1.475(4)
Cu−N(4)	2.295(2)	N(6)−C(11)	1.485(4)
Cu−N(5)	2.084(3)	C(1)−C(2)	1.520(5)
Cu−N(6)	2.108(3)	C(3)−C(4)	1.511(5)
N(1)−C(1)	1.473(4)	C(5)−C(6)	1.523(5)
N(1)−C(6)	1.474(4)	C(7)−C(8)	1.529(5)
N(1)−C(13)	1.478(4)	C(9)−C(10)	1.503(5)
N(2)−C(3)	1.470(4)	C(11)−C(12)	1.516(5)
N(2)−C(2)	1.485(5)	C(13)−C(14)	1.509(5)
N(3)−C(5)	1.480(4)	S−O(1)	1.471(2)
N(3)−C(4)	1.492(4)	S−O(2)	1.482(2)
N(4)−C(12)	1.474(4)	S−O(3)	1.471(2)
N(4)−C(7)	1.479(4)	S−O(4)	1.456(2)
N(4)−C(14)	1.484(4)		
N(1)−Cu−N(2)	79.32(10)	N(3)−Cu−N(6)	93.22(10)
N(1)−Cu−N(3)	79.37(10)	N(3)−Cu−N(4)	110.09(10)
N(1)−Cu−N(4)	76.23(9)	N(4)−Cu−N(5)	80.85(10)
N(1)−Cu−N(5)	110.17(10)	N(4)−Cu−N(6)	80.04(10)
N(1)−Cu−N(6)	150.78(10)	N(5)−Cu−N(6)	82.24(10)
N(2)−Cu−N(3)	82.04(10)	O(1)−S−O(2)	109.38(14)
N(2)−Cu−N(4)	149.87(10)	O(1)−S−O(3)	109.34(14)
N(2)−Cu−N(5)	91.43(10)	O(1)−S−O(4)	110.9(2)
N(2)−Cu−N(6)	128.01(10)	O(2)−S−O(3)	108.87(14)
N(3)−Cu−N(5)	167.36(10)	O(2)−S−O(4)	108.60(14)
		O(3)−S−O(4)	109.7(2)

Bridging two coordinated [9]aneN$_3$ moieties also affects the twist angle ϕ. This angle may be defined by the relationship of the N atoms of one ring to the other as viewed down the pseudo-C_3-axis. In perfect octahedral symmetry $\phi = 0°$, and for a trigonal prism where the projection of the N atoms of one ring are superimposed on the other, $\phi = 60°$. For example, calculations from X-ray crystallographic data for $[Cu([9]aneN_3)_2]^{2+}$ in crystals of $[Cu([9]aneN_3)_2](ClO_4)_2 \cdot 2H_2O$ show

Table 6. Selected Bond Distances (Å) and Angles (deg) for $[Cu(EM3)]ZnBr_4 \cdot H_2O$

Cu−N(1)	2.076(10)	C(7)−C(8)	1.48(2)
Cu−N(2)	2.402(9)	C(8)−N(5)	1.46(2)
Cu−N(3)	2.042(10)	N(5)−C(9)	1.48(2)
Cu−N(4)	2.098(10)	C(9)−C(10)	1.46(2)
Cu−N(5)	2.408(8)	C(10)−N(6)	1.47(2)
Cu−N(6)	2.056(9)	N(6)−C(11)	1.46(2)
N(1)−C(1)	1.44(2)	C(11)−C(12)	1.46(2)
C(1)−C(2)	1.52(2)	C(12)−N(4)	1.54(2)
C(2)−N(2)	1.50(2)	N(1)−C(13)	1.48(2)
N(2)−C(3)	1.46(2)	C(13)−C(14)	1.54(2)
C(3)−C(4)	1.50(2)	C(14)−C(15)	1.50(2)
C(4)−N(3)	1.53(2)	C(15)−N(4)	1.47(2)
N(3)−C(5)	1.51(2)	Zn−Br(1)	2.431(2)
C(5)−C(6)	1.44(2)	Zn−Br(2)	2.397(2)
C(6)−N(1)	1.47(2)	Zn−Br(3)	2.428(2)
N(4)−C(7)	1.48(2)	Zn−Br(4)	2.427(2)
N(1)−Cu−N(2)	79.8(4)	N(2)−Cu−N(6)	98.1(4)
N(1)−Cu−N(3)	83.0(5)	N(3)−Cu−N(6)	96.6(4)
N(2)−Cu−N(3)	78.5(4)	N(4)−Cu−N(6)	83.7(4)
N(1)−Cu−N(4)	96.8(5)	N(5)−Cu−N(6)	77.0(4)
N(2)−Cu−N(4)	107.1(4)	Br(1)−Zn−Br(2)	104.90(7)
N(3)−Cu−N(4)	174.3(4)	Br(1)−Zn−Br(3)	108.85(7)
N(1)−Cu−N(5)	105.0(4)	Br(1)−Zn−Br(4)	116.83(8)
N(2)−Cu−N(5)	172.6(4)	Br(2)−Zn−Br(3)	112.43(7)
N(3)−Cu−N(5)	167.3(1)	Br(2)−Zn−Br(4)	110.97(7)
N(4)−Cu−N(5)	78.1(3)	Br(3)−Zn−Br(4)	103.07(8)
N(1)−Cu−N(6)	177.9(4)		

Table 7. Selected Bond Lengths (Å) and Angles (deg) for $[Cu_2(EM2)Cl_4] \cdot 2H_2O$

Cu−N(1)	2.286(4)	N(2)−C(2)	1.486(6)
Cu−N(2)	2.040(4)	N(2)−C(3)	1.488(7)
Cu−N(3)	2.029(4)	N(3)−C(5)	1.486(7)
Cu−Cl(1)	2.306(1)	N(3)−C(4)	1.484(7)
Cu−Cl(2)	2.272(2)	C(1)−C(2)	1.517(7)
N(1)−C(6)	1.475(6)	C(3)−C(4)	1.506(8)
N(1)−C(1)	1.483(6)	C(5)−C(6)	1.535(7)
N(1)−C(7)	1.491(6)	C(7)−C(7)(#1)	1.513(10)[a]
N(1)−Cu−N(2)	82.1(2)	Cl(1)−Cu−N(3)	91.87(13)
N(1)−Cu−N(3)	83.5(2)	Cl(2)−Cu−N(1)	114.24(10)
N(2)−Cu−N(3)	82.2(2)	Cl(2)−Cu−N(2)	90.46(13)
Cl(1)−Cu−N(1)	100.00(11)	Cl(2)−Cu−N(3)	159.77(13)
Cl(1)−Cu−N(2)	173.50(12)	Cl(1)−Cu−Cl(2)	94.22(6)

[a] Symmetry transformation: $-x, -y, -z$.

Table 8. Bond Lengths (Å) and Angles (deg) for $[Cu_2(EM6)Cl_4]$

Cu−N(1)	2.271(4)	N(2)−C(2)	1.493(7)
Cu−N(2)	2.047(4)	N(3)−C(4)	1.478(7)
Cu−N(3)	2.049(4)	N(3)−C(5)	1.498(6)
Cu−Cl(1)	2.2803(14)	C(1)−C(2)	1.514(7)
Cu−Cl(2)	2.2752(14)	C(3)−C(4)	1.505(8)
N(1)−C(7)	1.468(6)	C(5)−C(6)	1.509(7)
N(1)−C(1)	1.481(6)	C(7)−C(8)	1.515(7)
N(1)−C(6)	1.482(6)	C(8)−C(9)	1.518(7)
N(2)−C(3)	1.480(7)	C(9)−C(9)[a]	1.497(9)
N(1)−Cu−N(2)	82.65(14)	N(2)−Cu−Cl(1)	164.94(12)
N(1)−Cu−N(3)	82.02(14)	N(2)−Cu−Cl(2)	90.55(13)
N(2)−Cu−N(3)	82.2(2)	N(3)−Cu−Cl(1)	90.23(12)
N(1)−Cu−Cl(1)	109.31(10)	N(3)−Cu−Cl(2)	170.88(12)
N(1)−Cu−Cl(2)	102.68(10)	Cl(2)−Cu−Cl(1)	95.48(6)

[a] Symmetry transformations used to generate equivalent atoms: $-x + 1, -y, -z$.

$\phi = 0 \pm 3°$.[19] For $[Cu(EM2)]^{2+}$ and $[Cu(EM3)]^{2+}$ the mean values of twist angle are 31 ± 3 and $6 \pm 13°$, respectively. These disparate values reflect the large differences in geometry of the CuN_6 polyhedra between these two complexes. The Cu−N(1) and Cu−N(4) bond distances and the N(1)−Cu−N(4) bond angles subtending the bridging groups of the complexes also vary considerably. For $[Cu(EM2)]^{2+}$ Cu−N(1) and Cu−N(4) are the longest bonds in the chromophore (2.35 and 2.30 Å), while the equivalent bonds in $[Cu(EM3)]^{2+}$ are 2.08 and 2.10 Å. The N(1)−Cu−N(4) angles bond are 76.2 and 96.8°, respectively. The combination of large twist angle, small N(1)−Cu−N(4) bond angle, and long Cu−N(1) and Cu−N(4) bond distances in $[Cu(EM2)]^{2+}$ reflects the strain placed on the complex by the ethylenic bridge. Although $[Cu(EM3)]^{2+}$ is considerably distorted (axial elongation) from the nonbridged $[Cu([9]aneN_3)_2]^{2+}$, it is apparent that the degree of trigonal twist distortion is greatly diminished from that for $[Cu(EM2)]^{2+}$.

Because of the smaller radius of Fe^{3+}, a smaller distortion in twist angle and corresponding bond angle and distances are observed for $[Fe(EM2)]^{3+}$ in crystals of $[Fe(EM2)]Br_3 \cdot 4H_2O$.[20] A Ni(II) complex containing two 10-membered NS_2 macrocyclic rings tethered by an ethylenic bridge also shows similar distortion.[21]

Structures of the two binuclear complexes $[Cu_2(EM2)Cl_4] \cdot 2H_2O$ (Figure 4) and $[Cu_2(EM6)Cl_4]$ (Figure 5) show similar coordination geometry to $[Cu_2(EMn)Cl_4]^{2+}$ ($n = 3, 4$)[4] and $[Cu([9]aneN_3)X_2]$ (X = Cl, Br).[22] The Cu−N and Cu−Cl bond distances and angles also fall into the range expected.[22] The Cu(II) is 5-coordinate and approximately square pyramidal in

Table 9. Absorbance Maxima (nm) and Extinction Coefficients ($dm^3\ mol^{-1}\ cm^{-1}$) for Cu(II) Complexes of EMn ($n = 2-6$) Ligands

	complex				
n	CuL^{2+}	$Cu_xL_x^{2x+1}$	CuH_2L^{4+}	Cu_2L^{4+}	$Cu_2L(OH)_2^{2+}$
2	648 (112)				
3	609 (64)[b]		643 (−)[a]	643 (116)	609 (156)
4		623 (67)[b,c]	650 (55)	650 (109)	623 (151)
5		586 (56)[c]	652 (53)	652 (106)	628 (185)
6		582 (50)[c]	650 (54)	650 (108)	626 (185)

[a] Measured at pH 3. [b] These are corrected wavelengths for those presented in ref 4 for $Cu(EMn)^{2+}$ ($n = 3, 4$). [c] Values of extinction coefficient per Cu(II).

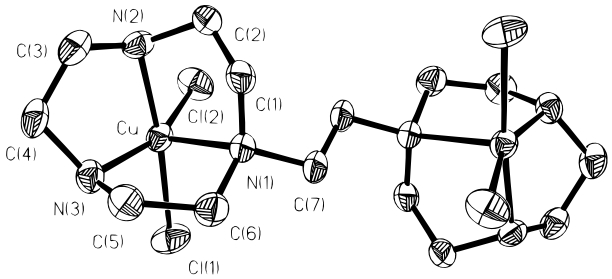

Figure 4. Thermal ellipsoid plot showing the structure of $[Cu_2(EM2)Cl_4]^{2+}$ in $[Cu_2(EM2)Cl_4] \cdot 2H_2O$ (**2**). Thermal ellipsoids are at the 50% probability level.

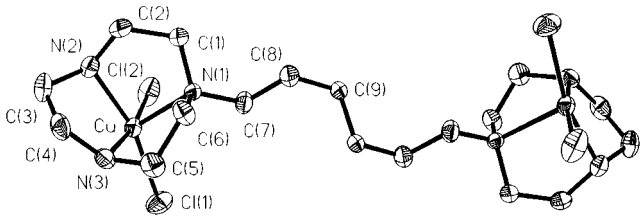

Figure 5. Thermal ellipsoid plot showing the structure of $[Cu_2(EM6)Cl_4]$ (**3**). Thermal ellipsoids are at the 50% probability level.

(19) Beveridge, A.; Lavery, A.; Walkinshaw, M.; Schröder, M. *J. Chem. Soc., Dalton Trans.* **1987**, 373.

(20) Geilenkirchen, A.; Wieghardt, K.; Nuber, B.; Weiss, J. *Naturforsch.* **1989**, *44B*, 1333.

(21) Chandrasekhar, S.; McAuley, A. *Inorg. Chem.* **1992**, *31*, 2234.

(22) (a) Bereman, R.; Churchill, M.; Schaber, P.; Winkler, M. *Inorg. Chem.* **1979**, *18*, 3122. (b) Schwindinger, W.; Fawcett, T.; Lalancette, R.; Potenza, J.; Schugar, H. *Inorg. Chem.* **1980**, *19*, 1397.

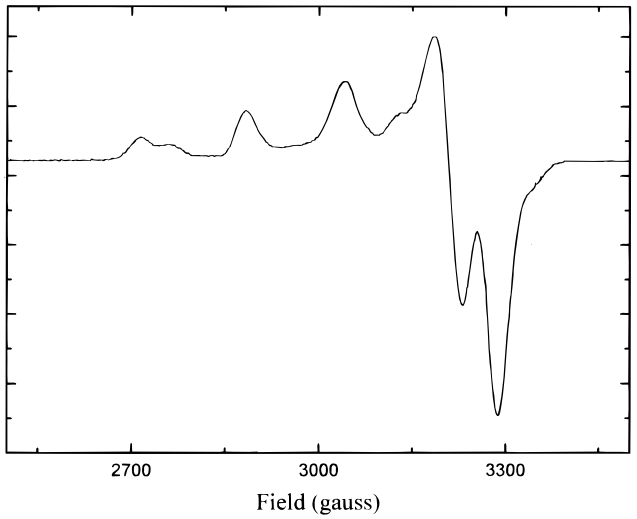

Figure 6. X-band EPR of $[Cu(EM2)]SO_4$ in H_2O/DMSO (1:1) at 100 K.

shape. The base of the pyramid is formed by the two Cl ions and secondary amine N atoms (N(2) and N(3)). The apex is occupied by the tertiary amine N atom (N(1)) with the axial (Cu−N(1)) bond distance averaging 0.24 Å longer than the Cu−N bond distances in the basal plane. For $[Cu_2(EM2)Cl_4]\cdot 2H_2O$ and $[Cu_2(EM6)Cl_4]$ respectively the mean deviation from the plane of atoms forming the base is 0.14 and 0.07 Å, and the Cu(II) extends 0.21 and 0.19 Å into the pyramid. In both structures the Cl ions assume an *anti* conformation. Thus, for even numbers of C atoms in the bridging chain the Cl ions are *anti* and for odd they are *syn*.[4] The Cu···Cu nonbonded distances in the dimers are 6.7 and 11.6 Å for $[Cu_2(EM2)Cl_4]\cdot 2H_2O$ and $[Cu_2(EM6)Cl_4]$, respectively. Tables 7 and 8 contain bond distances and angles for the dicopper(II) complexes.

EPR Studies. The X-band EPR spectra (Figure 6) were measured on frozen solutions (H_2O/glycerol (1:1) or H_2O/DMSO (1:1)) of $[Cu(EM2)]SO_4$ at about 100 K. The spectra are similar in each frozen solution. Some features at the low-field side of the spectra suggest the presence of more than one Cu(II) species in solution. This may mean the that the complex is trapped in more than one conformation in the rigid matrix. Because of the unresolved features, the magnetic parameters could not be determined with high precision. Approximate values determined with the aid of spectrum simulations are $g_{\|} = 2.225$, $g_{\perp} = 2.045$, $A_{\|} = 164 \times 10^{-4}$ cm^{-1}, and $A_{\perp} \approx 0$ cm^{-1}.[23] The spectra are characteristic of axially symmetric Cu(II) complexes. However, a rhombic distortion may be hidden because of the broad lines which likely result from unresolved ^{14}N hyperfine structure.

Q-band EPR spectra were obtained from frozen solutions (H_2O/DMSO) of $Cu(EM2)^{2+}$ at 86 K. The spectrum could be simulated with $g_{\|} = 2.227$, $g_{\perp} = 2.064$, $A_{\|} = 155 \times 10^{-4}$ cm^{-1}, $A_{\perp} \approx 0$ cm^{-1}, and line widths ranging from 25 G for the parallel region to 37 G for the perpendicular region. The line widths, in part, reflect the hyperfine couplings with ligand nuclear spins (^{14}N). In the perpendicular region the line widths are also due to some unresolved Cu hyperfine splitting. In the Q-band spectrum there is a broad resonance in the low-field (parallel) region. This again appears to indicate that the complex freezes out in two different conformations.

(23) Rigid-matrix EPR spectra were simulated with the EPRPOW program provided by Prof. Dennis Chasteen of the University of New Hampshire. The program is a PC adaptation of the program developed by L. K. White and described in: Electron Paramagnetic Studies of Copper(II) Complexes. PhD Thesis, University of Illinois, Urbana, IL, 1975.

Conclusions

The series of "earmuff" ligands containing two to six C atom bridging chains form a wide variety of Cu(II) complexes both in solution and the crystalline solid. The smaller chain ligands, where $n = 2$ or 3, form very stable mononuclear, CuL^{2+}, complexes in solution and in the crystal. All ligands except EM2 form stable binuclear, Cu_2L^{4+}, species in aqueous solution, and crystalline solids of binuclear complexes containing $[Cu_2(EMn)Cl_4]$ are obtained with all the ligands. Ligands with bridging chains of four or more C atoms appear to form stable 1:1 dimeric or oligomeric species in solution. Although no structures have been determined for these complexes, it is believed that Cu(II) ions are shared by [9]aneN_3 complexing groups from different ligands. In aqueous solution at pH > 7 the binuclear complexes hydrolyze to form complexes with $Cu_2L(OH)_2^{2+}$ stoichiometry.

The trends in stability of the 1:1 complexes in aqueous solution follow those expected for chelating ligands. Ligands capable of forming five- or six-membered chelate rings through their bridging groups (EM2 and EM3) form the most stable Cu(II) complexes. When the bridging group of the ligand is extended beyond three C atoms, it appears that somewhat less stable dimeric or oligomeric species form. Binuclear, Cu_2L^{4+}, and protonated mononuclear, CuH_2L^{4+}, complexes show virtually no change in stability as the C chain is lengthened from three to six atoms. The same is true for the hydrolyzed species.

The UV−vis spectroscopic properties of the various complexes can be explained by the equilibrium models employed. Because of the conformational rigidity of the [9]aneN_3 group, there is apparently considerable similarity between the chromophoric groups of the CuH_2L^{4+} and Cu_2L^{4+} species in solution.

Recently it was discovered that Cu([9]aneN_3)Cl_2 hydrolyzes proteins[24] and cleaves single-stranded and double-stranded DNA.[25] The bridged dimers of this compound reported here might also be expected to show such activity and include an added dimension of a variable length bimetallic reaction center.

Acknowledgment. The authors thank Dr. Nancy Lenhoff of Polaroid Corp., Cambridge, MA, for assistance in the CV electrochemical experiments. We also thank Prof. Hans van Willigen of the University of Massachusetts Boston and Professor Dennis Chasteen of the University of New Hampshire for assistance in acquiring EPR spectra and helpful discussions. The donors of the Petroleum Research Fund, administered by the American Chemical Society, are gratefully acknowledged for partial support of this work.

Supporting Information Available: Four X-ray crystallographic files, in CIF format, are available on the Internet only. Access information is given on any current masthead page.

IC970070F

(24) Hegg, E.; Burstyn, J. *J. Am. Chem. Soc.* **1995**, *117*, 7015.
(25) Hegg, E.; Burstyn, J. *Inorg. Chem.* **1996**, *35*, 7474.